ELSEVIER

0951-8339(95)00030-5

Marine Structures 9 (1996) 449–470
Elsevier Science Limited
Printed in Great Britain.
0951-8339/96/$15.00

Approximate Method to Evaluate the Hull Girder Collapse Strength

J. M. Gordo & C. Guedes Soares

Unit of Marine Technology and Engineering, Technical University of Lisbon, Instituto Superior Técnico, Av. Rovisco Pais, 1096 Lisboa, Portugal

ABSTRACT

A method to estimate the ultimate moment based on a simplified approach to represent the collapse strength of beam columns is presented. Comparisons with experimental results of box girders, small scale models of box girders and a 1/3 frigate model are performed. Also, a comparison with results of other approximate methods and finite elements codes is made.

Key words: collapse strength, plate structures, hull girders.

NOTATION

A_i	Sectional area of element i
C	Curvature
C_x	Curvature over x axis
C_y	Curvature over y axis
E	Young's modulus of the material
E_i	Tangent modulus of the element i
l	Length between frames
M	Magnitude of the bending moment
M_x	Component of the moment about x axis
M_y	Component of the moment about y axis
NL	Net load of the section
r	Radii of gyration of the cross section of the element
x_{gi}	Horizontal distance of the centroid element i to the instantaneous CG
x_i	Distance of the centroid of element i to the center line

x_n Instantaneous abcissa of the centroid of area
y_{gi} Vertical distance of the centroid of element i to the instantaneous CG
y_i Distance of the centroid of element i to the base line
y_n Instantaneous ordinate of the centroid of area
ε_i Strain of element i
ε_o Yield strain
η Width of the tensile zone due to residual stresses normalised by the thickness
λ column slenderness $= \frac{l}{r}\sqrt{\frac{\sigma_o}{E}}$
σ_i Average stress in element i
$\bar{\sigma}_n$ Normalised residual stress
θ Angle between the vector of curvature and the x axis
$\Phi(\varepsilon_i)$ Average stress of element i at a strain of ε_i normalised by the yield stress
ΔNA Shift of the neutral axis

1 INTRODUCTION

The ultimate or maximum bending moment of the ship cross section represents an important item of information required to design the primary structure of ships. The philosophy of designers and Classification Societies is nowadays changing and more attention is devoted to the whole range of the moment-curvature relationship of the ship hull especially the post-buckling behaviour and the differences between sagging and hogging ultimate moment.

The profession has been aware of these failure modes for a long time, as can be noted from the early contribution of Caldwell.[1] However it has been only with the developments in non-linear finite element codes[2,3] and with approximate methods to represent the load-shortening behaviour of plates[4,5] and stiffened plates[6,7] that major advances have been seen in this topic.

Historically, the earliest attempts to incorporate plate buckling and its effects on ship strength were made by Caldwell[1] using a simplified procedure where the ultimate moment of a mid-ship cross section in the sagging condition was calculated introducing the concept of a structural instability strength reduction factor for the compressed panels. This factor would account for the reduced strength of the cross section due to early failure and unloading of some plate elements.

Smith[2] developed a method to incorporate the load shortening curves of the plate elements in the calculation of the hull girder collapse. The

behaviour of each plate was calculated by finite-elements and their contribution to the overall behaviour of the girder was accounted as a function of the plate location in the cross section. Other methods based on the same general approach were afterwards developed, including the simplified approaches by Billingsley,[8] Adamchak[9] and Dow *et al.*[10]

Rutherford and Caldwell[11] presented recently a comparison between the ultimate bending moment experienced by a VLCC and the results of strength calculations in which a simplified approach to stiffened plate strength was used, without considering their post-buckling strength. The importance of lateral pressure, initial deformations and corrosion rates were also investigated. The validity of the method and model was confirmed by comparing with the results of a nonlinear finite element program.

More accurate approaches have been applied by Chen *et al.*,[12] based on a non-linear finite element method but it was shown to be very time consuming both in data preparation and in computation time. This indicated that a simplified approach was required and this is the main motivation for this work.

The general approach of calculating the load shortening curve of the hull girder from the contribution of each element is similar to the ones adopted in Refs 2, 8–11. The main difference is in the model of the behaviour of each of the main elements of the hull i.e. the plate stiffener assembly which is modelled as described in Ref. 13. The approach has been presented in Ref. 14 where it was compared with the results of Rutherford and Caldwell[11] and its usefulness was demonstrated in various studies related to the design of the primary structure. In this work the method is applied to further test cases in order to validate it against experimental results.

2 MOMENT–CURVATURE CURVES

The present method follows the general approach presented initially by Smith[2] and later by others[8–11] for the contribution of each element to the hull strength, but the model adopted in this work to represent plate strength and beam–column behaviour were reported in Ref. 13.

2.1 The method

Broadly speaking, the assessment of a moment–curvature relationship is obtained from the imposition of a sequence of increasing curvatures to the hull's girder. For each curvature, the state of average strain of each beam–column element is determined. Entering these values in the model that represents the load-shortening behaviour of each element, the load that it

sustains is calculated and consequently the bending moment resisted by the cross section is obtained from the summation of the contributions from the individual elements. The derived set of values defines the desired moment–curvature relation.

However, some problems arise in this implementation, because the sequence and the discretisation of the sequence of the imposed curvatures strongly influences the convergence of the method due to the shift of the neutral axis. In this method, the modelling of the ship's section, which will be treated in Section 2.2, and the determination of the position of the neutral axis are important issues, as has already been pointed out in Ref. 14.

The basic assumptions of the method are:

— the elements, composed of longitudinal stiffeners and an effective breadth of plate into which the cross section is subdivided, are considered to act and behave independently;
— the ship cross section is assumed to be plane and to remain plane when its curvature is increasing;
— the overall grillage collapse of the deck and bottom structures is avoided by using sufficiently strong transverse frames.

As a first step it is necessary to estimate the position of the neutral axis through an elastic analysis, because when the curvature is small the section acts in the elastic domain. The elastic neutral axis passes through a point with coordinates given by:

$$\begin{cases} x_n = 0 \\ y_n = \dfrac{\sum y_i A_i}{\sum A_i} \end{cases} \tag{1}$$

if the section is symmetric and the origin of the reference system is located on the baseline, Fig. 1. The meaning of the symbols is indicated in the notation section.

The most general case corresponds to that in which the ship is subjected to curvature in the x and y directions, respectively denoted as C_x and C_y. The global curvature C is related to these two components:

$$C = \sqrt{C_x^2 + C_y^2} \tag{2}$$

or:

$$\begin{cases} C_x = C \cdot \cos\theta \\ C_y = C \cdot \sin\theta \end{cases} \tag{3}$$

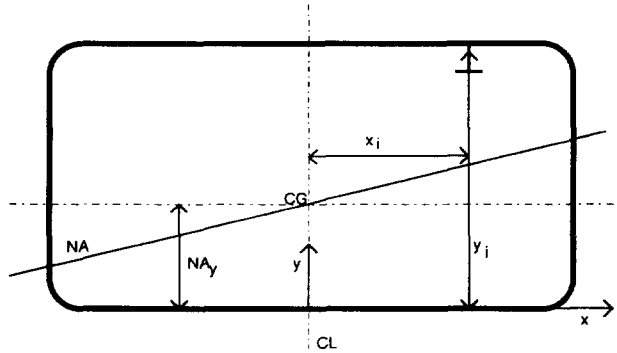

Fig. 1. Combined bending of the hull girder.

adopting the right-hand rule, where θ is the angle between the neutral axis and the x axis. The strain at the centroid of an element i is ε_i which depends on its position and on the hull curvature, as given by:

$$\varepsilon_i = y_{gi} \cdot C_x - x_{gi} \cdot C_y \tag{4}$$

or, substituting (3) in (4):

$$\varepsilon_i = C \cdot (y_{gi} \cdot \cos\theta - x_{gi} \cdot \sin\theta) \tag{5}$$

where (x_{gi}, y_{gi}) are the coordinates of the centroid element i (stiffener and associated effective plate) referred to the point of the intersection of the neutral axis and the center line. The relations between these local coordinates and the global coordinates are:

$$x_{gi} = x_i - x_n \tag{6}$$

$$y_{gi} = y_i - y_n \tag{7}$$

Equations (6) and (7) are still valid if one uses any point belonging to the neutral axis instead of the point used before.

Once the state of strain in each element is determined, the corresponding average stresses may be calculated according to the method described in Ref. 8 and consequently the components of the bending moment for a curvature C are given by:

$$\begin{cases} M_x = \sum y_{gi} \cdot \Phi(\varepsilon_i) \cdot \sigma_o A_i \\ M_y = \sum x_{gi} \cdot \Phi(\varepsilon_i) \cdot \sigma_o A_i \end{cases} \tag{8}$$

where x_{gi} and y_{gi} are the distances from the element i to the local axes of a reference system located in the precise position of the instantaneous 'center of gravity' (CG), and $\Phi(\varepsilon_i)$ represents the non-dimensional strength of the

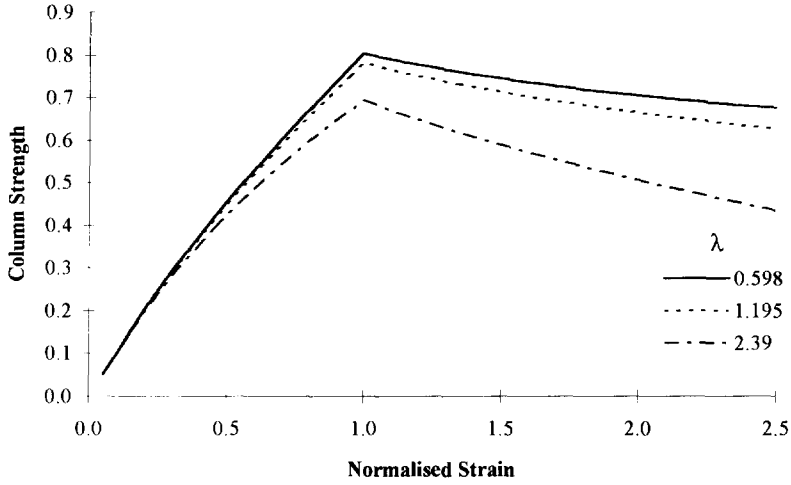

Fig. 2. Load shortening curves of stiffened plates with plate slenderness of 2.32 and different column slendernesses, λ.

element as a function of the strain ε_i, i.e., the average stress of the stiffened plate element normalised by the yield stress, which has an appearance like the examples in Fig. 2.

The load shortening curve is controlled by two main parameters which are the effective plate slenderness and the effective column slenderness. These slendernesses are associated with the geometry of the stiffened element and its mechanical properties like the nominal slendernesses, but they are also related to the average strain state. Thus, with the increase of compressive strain a loss of effectiveness of the plate may be felt once the effective slenderness exceeds unity. The very stocky plates do not have any loss of rigidity in the pre-collapse region and they may sustain stresses near the yield stress up to very large plastic strains. On the other extreme, very slender plates lose structural rigidity at an early stage of the loading process and they show a more pronounced load shedding after collapse than the stocky ones.

The most marked shedding after collapse is exhibited by the plates of intermediate slenderness because in these plates the variation of effective width with the slenderness has an absolute minimum. These changes in the effective width of the plate during the loading process have a direct repercution on the column slenderness through the calculation of the effective moment of inertia.

The modulus of the total bending moment is:

$$M = \sqrt{M_x^2 + M_y^2}. \tag{9}$$

This is the bending moment on the cross section if the assumed instantaneous position of the center of gravity is correct. However, during the stepwise process of increasing the hull's curvature, the location of the center of gravity is shifting and it becomes necessary to calculate the shift between two imposed curvatures. Rutherford and Caldwell[6] suggested that the shift could be taken equal to:

$$\Delta NA = \frac{\sum (A_i \cdot \sigma_i)}{C \cdot \sum (A_i \cdot E_i)} \tag{10}$$

but, in this work, it was felt that this expression underestimated the shift and may cause problems in convergence.

For this reason a trial-and-error process was implemented, having as stopping criteria one of the two conditions: the total net load in the section, NL, or the error in the shift estimation ΔNA should be less than or equal to a sufficiently low value. Equations (11) and (12) represent analytically these two conditions, where ξ was taken equal to 10^{-6}.

$$NL = \sum (\sigma_i \cdot A_i) \leqslant \xi \cdot \sigma_o \cdot \sum (A_i) \tag{11}$$

$$\Delta NA = k_E \cdot \frac{NL}{C \cdot E \cdot \sum A_i} \leqslant 0.0001. \tag{12}$$

The factor k_E is a function of the curvature and yield strain introduced to allow a better convergence of the method, and it is a result of the variation in the structural tangent modulus of the overall section with curvature.

2.2 Modelling of the ship's cross section

The modelling of the ship's cross section consists of discretising the hull into stiffened plate elements which are representative of panel behaviour. Most of the present day ships have longitudinally stiffened hulls. In this kind of hull, it is common practice to have large panels with similar and repetitive properties such as space between stiffeners, thickness and stiffener geometry.

As the behaviour of these panels may be represented as the behaviour of n equally stiffened plate elements, the hull section will be divided into small elements representing a plate between stiffeners and the corresponding stiffener. Apart from the validity of this model as concerns the panel behaviour, already discussed in Ref. 13, some other points of the modelling present some problems or approximations, especially related to:

— the validity of the element's stress state as derived from the strain state at the centroid of the element,

— the modelling of side girders when web stiffeners are not present,
— the modelling of the corners of the hull girder,
— the modelling of large and reinforced flanges of the primary longitudinal girder system and the validity of this subdivision on the overall behaviour of main girders, specially relating to sideways flexural behaviour.

Relating to the first point, Fig. 3 shows the strain distribution along the depth of a reinforced element. The stress state of the components of the element (plate and stiffener) is computed considering the strain at the centroid ε_i. However the strain of the real plate is higher than this and is approximately equal to ε_{max}. This error is only relevant when the element belongs to horizontal panels, such as deck and bottom. In these two structures the distance of the elements from the neutral axis is large compared with the dimensions of the elements, which results in a ratio between these two strains close to one, making the approximation acceptable and allowing the simplification of the procedures and iterations.

In this work the girders are modelled considering three main components: the flange with a stiffener, which is not more than the edge of the girder's web, another stiffened plate on the other side of girder consisting of side plating and part of the web, and a central plate region, Fig. 4. The extremes are modelled as beam–columns in order to compute their higher rigidity

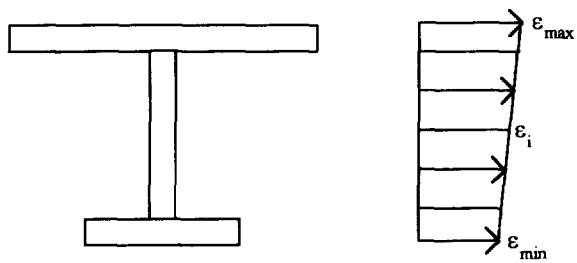

Fig. 3. Strain state of a stiffened plate element.

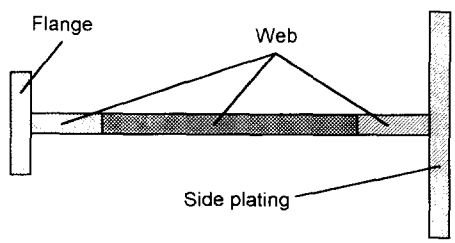

Fig. 4. Modelling of unstiffened side girders.

compared with that of plate elements alone. The breadth of the stiffeners which is part of the web must be carefully chosen by the designer in such a way that they behave as hard corners, i.e., low nominal column slenderness. The contribution of the central plate element is calculated approximately by the curve for transversely loaded plates, as derived in Ref. 14.

As regards the contribution of the corners, normally three situations are considered: first, behaving like hard-corners, i.e., considering that their strength is one ($\Phi = 1$) in the plastic domain, second, not taking into account any contribution of the corners on hull's strength, or modelling corners like usual beam–columns. Any of these solutions is formally unsatisfactory because they do not include the influence of the buckled state of adjacent panels on the behaviour of the corner, but they represent limit cases that bound the real one.

3 CORRELATION WITH EXPERIMENTAL RESULTS

The accuracy of the method just described was assessed from comparison with experimental results performed by different authors. Two models from Dowling *et al.*,[15,16] seven models from Nishihara[17] and a model of a frigate from Dow[18] were chosen as the test cases.

3.1 Dowling tests

The models were single box girders with a width of 1219.2 mm and a depth of 914.4 mm. The span of the stiffeners between frames was 787.4 mm (see Figs 5 and 6).

The plating of Model 2 was reinforced by equal L stiffeners of

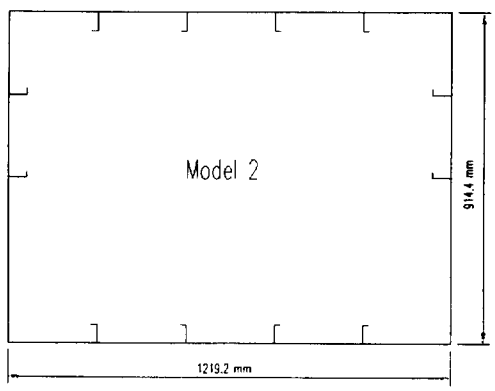

Fig. 5. Model 2 of Dowling *et al.*[15]

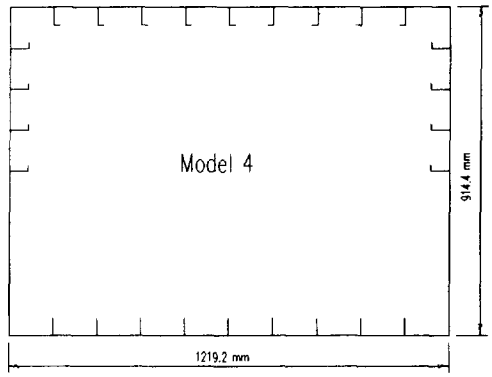

Fig. 6. Model 4 of Dowling *et al.*[15]

50.8 × 4.76 mm by 15.9 × 4.76 mm. The compression and tension flanges were made of 4.86 mm plate thickness while the side flanges were 3.36 mm thick.

An important aspect of this model is the difference in the material properties between the plate and the stiffeners. In the compression and tension flanges the plating had a yield stress of 297.3 MPa and Young's modulus of 208.5 GPa, while the stiffeners had values of 276.2 MPa and 191.5 GPa, respectively. In the side flange the yield stress of the plating was 211.9 MPa and the Young's modulus was 216.2 GPa, while the stiffener had values of 276.2 MPa and 191.5 GPa, respectively.

The stiffener spacing in the flanges was 241.3 mm which corresponds to a plate slenderness of 1.875, this value being similar to those found in merchant ships. The column slenderness of the top flange panel is $\lambda = 2.02$, where λ is defined in the notation according to the definition of column slenderness in Ref. 13, i.e., considering the effective width of plate for the radii of gyration of the section.

Figure 7 shows the moment–curvature relationship and the associated shift of the neutral axis. As may be noted the buckling of the cross-section is very well marked at a curvature of about 3.2×10^{-3} m^{-1} and a sharp decrease in the position of the neutral axis starts at this point.

The stiffener behaviour of the compression panel is shown in Fig. 8, where a comparison is made between the predicted behaviour with and without residual stresses. In Ref. 15 it is indicated that the level of residual stresses during the test was of $0.2\sigma_0$.

The effect of assuming a non-zero value for residual stresses is specially noted in the ultimate strength of the panel and the difference may be as large as 10%. In this particular case the ultimate strength of the panel without residual stresses is 0.755 while with 20% residual stresses it is 0.671. For

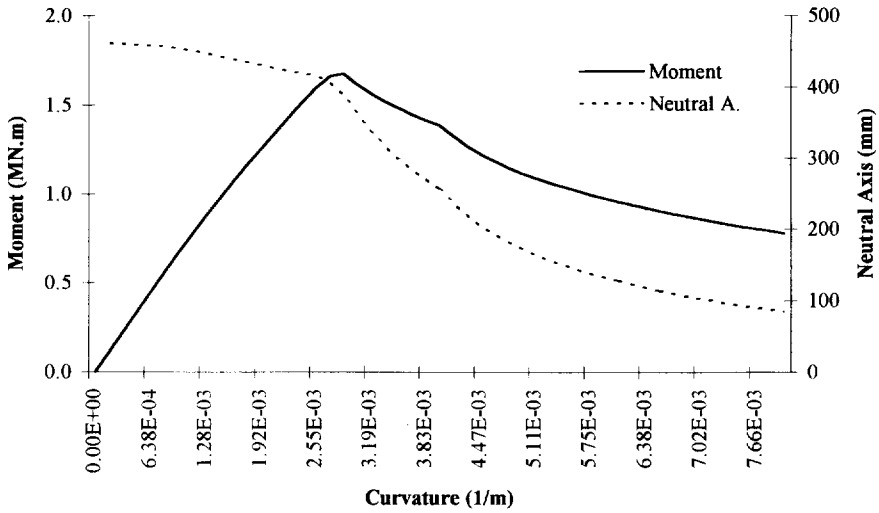

Fig. 7. Moment–curvature curve of Model 2 and corresponding position of the neutral axis in the upright position (top flange in compression) using the average stress as element yield stress.

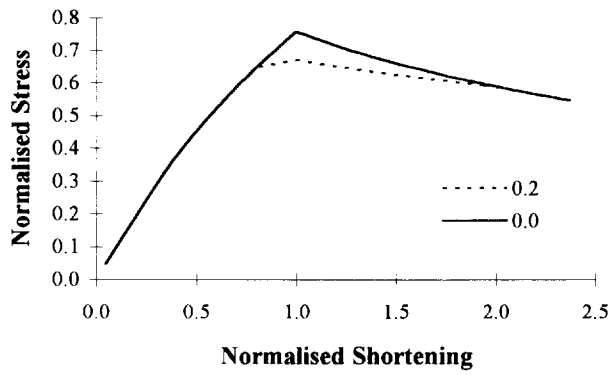

Fig. 8. Behaviour of the compression panel of Model 2 and its dependence on residual stresses ($\bar{\sigma}_r = 0.0$ and 0.2) using a value of 293.4 MPa for the yield stress.

large end shortenings the differences between the curves tend to reduce and from a level of $\varepsilon = 2{\cdot}\varepsilon_o$ the prediction is the same regardless of the level of residual stresses.

The effect of the residual stresses on the moment–curvature curve is shown in Fig. 9. Three levels of residual stresses are considered, as the stresses that equilibrate the two areas with tensile yield stresses at the edges of the plate with widths of 0, 2 and 4 times the plate thickness. In the top flange plating, this corresponds to values of $\bar{\sigma}_r = 0.0$, 0.09 and 0.19, respectively, reminding

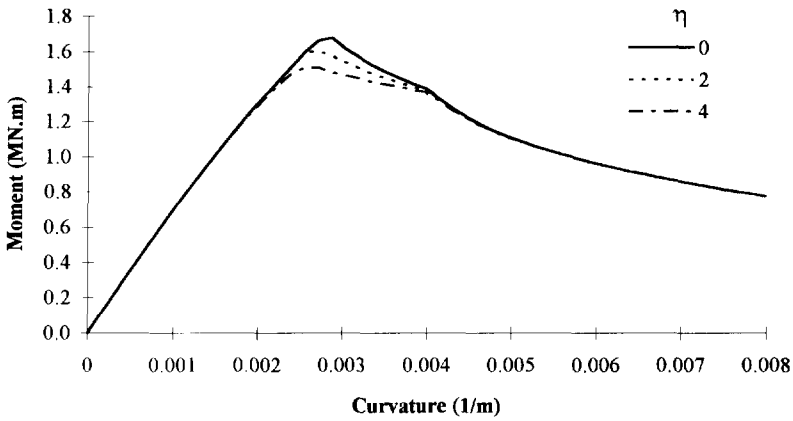

Fig. 9. Moment–curvature relationship of Model 2, considering three levels of residual stresses (η) and an average yield stress.

us that the average level of residual stresses in the experiment was 0.176. The decrease in load carrying capacity is only relevant near the collapse load and it tends to smoothen the load shortening curve in that region. The predicted ultimate moment for each level of residual stresses is summarized in Table 1, where the results for two values of the yield stress are compared with the one obtained in the experiment.

Figure 10 compares the curves obtained when one uses the minimum yield stress of the stiffener and the plate instead of the average yield stress. As may be noticed, the ultimate moment is reduced, as expected, and also the rigidity of the model is lower. However, the ultimate moment is reached at approximately the same curvature in both cases.

Model 4 is similar to Model 2 but has a closer spacing between stiffeners, in fact half of the Model 2 stiffener spacing (120.65 mm). The plating is

TABLE 1

Summary of Model 2 Results, Defining the Yield Stress of the Plate Stiffener Assembly as the Average or the Minimum Value Between the Two. The Value of M_{ap} Corresponding to a Residual Stress Ratio of 0.176 was Calculated by a Linear Interpolation

Bending moment (MN.m)	*Residual str.*	*Average stress*	*Minimum stress*
Fully plastic	–	2·276	2·059
	0·0	1·660	1·514
Approximate method (M_{ap})	0·087	1·589	1·459
	0·192	1·507	1·385
Experimental (M_{exp})	0·176	1·543	1·543
M_{ap}/M_{exp}	0·176	98·5%	90·5%

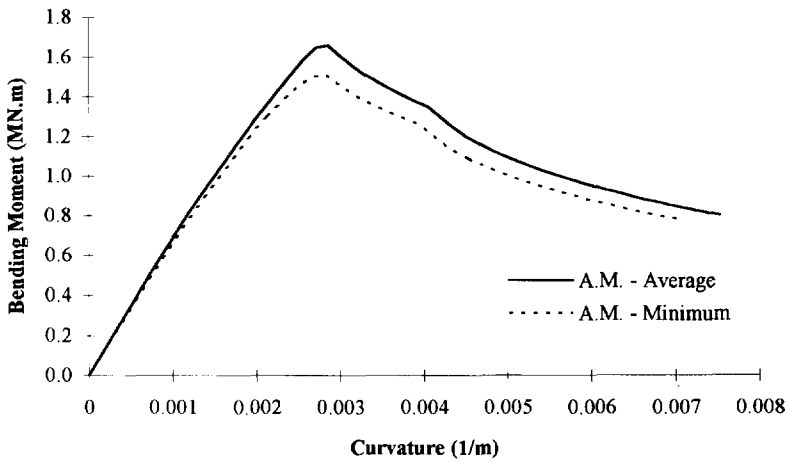

Fig. 10. Moment–curvature relationship of Model 2 using the minimum yield stress and the average yield stress between the stiffener and the plate without considering residual stresses.

slightly thicker than in Model 2, i.e., 5.02 mm in the compression flange and 4.94 mm in the remainder, and the yield stress is 221.0 MPa in the compression flange, 215.6 in the tension flange and 280.6 in the side plating. The modulus of elasticity is 207 GPa, 208.7 and 214.1 respectively. The plate slenderness, in the compression flange, is 0.79.

The stiffeners in the compression and side flanges have the same geometry as in Model 2 but the series has different material properties, i.e., 287.9 MPa for yield stress and 199.2 GPa for Young's modulus. The stiffeners in the tension flange were bars with dimensions 50.8 × 6.35 mm with a yield stress of 303.8 MPa and a Young's modulus of 206.2 GPa. The column slenderness is 1.54 in the compression and side flanges.

The results for the ultimate bending moment of this model are summarized in Table 2 and compared with the experiment. The main conclusions are, first, the insensitivities of the ultimate moment to the level of residual stresses, which is a direct consequence of the plate slenderness ($\beta = 0.79$). For this kind of plate the failure is due to plastic collapse and not to buckling in which case residual stresses are not relevant. The second conclusion is the good agreement between the predictions and the experiment, within a range of 10%. However, it should be noted that the experimental and the numerical results are closer to each other when the minimum yield stress is used.

Figure 11 plots the moment–curvature relationships for several levels of residual stresses, where the width of the yield zone $\eta = 2$ and 4 corresponds to $\bar{\sigma}_r = 0.2$ and 0.5, respectively. The flatness of the curves is, again, due to the plate slenderness and also due to a less slender column. In the pre-

TABLE 2
Summary of Model 4 Results, Defining the Yield Stress of the Plate Stiffener Assembly as the Average or the Minimum Value Between the Two

Bending moment (MN.m)	*Residual str.*	*Average stress*	*Minimum stress*
Fully plastic	–	2·668	2·452
	0·0	2·466	2·248
Approximate method (M_{ap})	0·2	2·447	2·233
	0·5	2·419	2·206
Experimental (M_{exp})	0·562	2·212	2·212
M_{ap}/M_{exp}	0·562	1·091	0·995

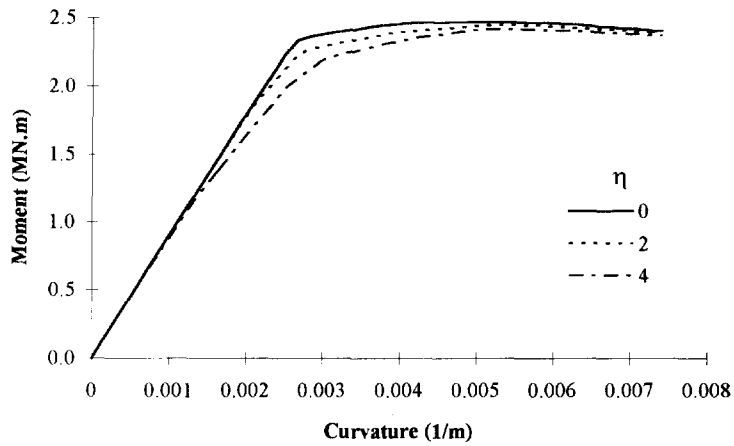

Fig. 11. Moment–curvature relationship of Model 4, considering three levels of residual stresses (η) and adopting the average yield stress between plate and stiffener.

collapse region the increase of residual stresses corresponds to less rigid box girders.

The choice of the yield stress is only important as a scale factor for girders with this level of plate and column slenderness, Fig. 12. The behaviour in the elastic region is the same in both cases and the curves only diverge at a point corresponding to the yielding of the compression flange for the minimum yield stress.

3.2 Nishihara tests

Nishihara[7] tested nine box girder models of four typical ships under pure bending moments. The models had cross-sections with overall dimensions of 720 × 720 mm and 900 mm long, representing tankers without double bottom (MTS-3 and MST-4), with double bottom (MSD), bulk carriers

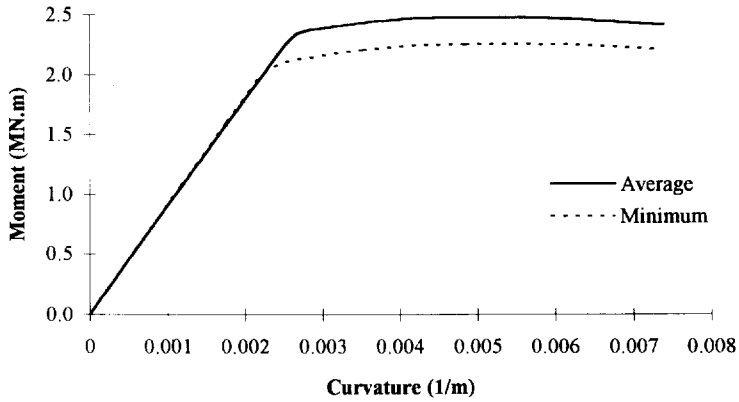

Fig. 12. Moment–curvature relationship of Model 4, using the average stress and the minimum yield stress.

(MSB) and container ships (MSC). The difference between the models MST-3 and MST-4 is the thickness of the plating, 3 and 4.3 mm, respectively. The spacing between frames was 540 mm for all models.

The frames and the longitudinal stiffeners were made of bars 90 mm and 50 mm wide, respectively, of 3 mm thickness, except in model MST-4 in which it was 4.3 mm. The wing tanks of the model MSC were made of plate of 5.6 mm thickness.

Table 3 compares the ultimate bending moments experienced by the models and those predicted with the approximate method. The experimental values are all within the predictions with and without accounting for tripping, except for the container ship model in sagging. In this case it seems

TABLE 3
Summary of the Comparison with the Results of the Nishihara Tests Without Considering Residual Stresses

Model	*Condition*	*Experiment (KN.m)*	*Prediction (KN.m)*		*Ratio (pred/exp)*	
			Tripping	*Fl. buck.*	*Tripping*	*Fl. buck.*
MST-3	Sag = Hog	564	512	634	0·908	1·124
MST-3	Sag = Hog	588	512	634	0·871	1·078
MST-4	Sag = Hog	926	909	909	0·982	0·982
MSD	Sag	593	549	672	0·926	1·133
MSD	Hog	838	780	861	0·931	1·027
MSC	Sag	1112	945	970	0·850	0·872
MSC	Hog	862	769	917	0·892	1·064
All	All	—	—	—	0·909	1·040

that one must model the wing tanks as hard corners instead of columns, to be able to obtain adequate results.

For the other cases, it seems that the tripping formulations are a little conservative, on the order of 10%, and they may be used as a lower bound while the formulation without tripping may be used as an upper bound. In the case where tripping as not detected (MST-4) both predictions are coincident and very close to the experiment.

3.3 Dow experiment

Dow[8] tested a 1/3-scale model representing a typical warship hull structure subjected to a sagging bending moment. The overall dimensions of the model were $18\,\text{m} \times 4.1\,\text{m} \times 2.8\,\text{m}$. Detailed information about the initial imperfections and residual stresses was collected during the construction. Concerning the residual stresses in the model, one has to note its very large magnitude ($\bar{\sigma}_r = -0.543$, on the average) and, more important than that, the large scatter (COV = 0.49). However, it is important to realize that this is the type of variability that has been reported earlier,[19] indicating that the conditions of the experiment were representative ones. To perform deterministic calculations it is necessary to fix the value of residual stresses and thus the results obtained by applying only one or two levels of residual stresses have to be judged carefully.

Figure 13 plots the results obtained with the approximate method compared with a set of experimental points.[18] The general agreement is good and the estimated ultimate bending moment is very close to that experienced by the model. The influence of residual stresses in this particular section is not of considerable importance on the ultimate moment and post-buckling behaviour. The differences between the moment–curvature curves at normal levels of residual stresses ($\eta < 4$) are only relevant for curvatures lower than the ultimate curvature.

The main differences are observed in the pre-buckling state. It is also in that region that the disagreement between the test and the prediction is larger, especially in that concerning the rigidity of the section (between curvatures 0.0006 and 0.0012/m). However similar behaviour in this range of curvatures was obtained by Dow[18] using a finite element code as well as by Yao & Nikolov[20] with another similar method, both based on Smith's method.[2] This behaviour is predicted as a result of the yielding in tension of the elements near the keel, because the distance from the keel to the elastic neutral axis is greater than from the deck to that axis. Dow remarks that this disagreement may be the result of 'the computation of the experimental curvature of the hull from the measured vertical displacements'.[18]

The predictions shown in Table 4 were obtained considering only the

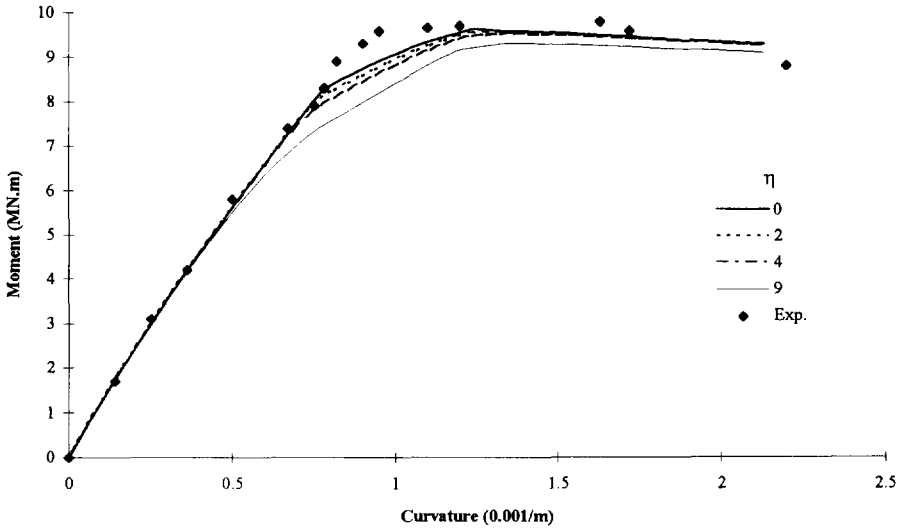

Fig. 13. Dow experiment on a frigate model. Comparison between the prediction for several tensile widths η and the experimental results.

TABLE 4

Dow Test of 1/3 Model Frigate. Summary of Results with Indication of the Level of Residual Stresses for the Deck In board (2 mm) and Deck Outboard and Side Shell (3 mm). The Experimental Value is Evaluated from Ref. 18, figure 12

Method/analysis	$\eta(\bar{\sigma}_r)$	*Bending moment (MN.m)*
Fully plastic	—	13·02
Approximate method (M_{ap})	0 (0·0, 0·0)	9·63
	2 (0·04, 0·06)	9·56
	4 (0·09, 0·13)	9·51
	9 (0·21, 0·36)	9·31
Experimental (M_{exp})	~13 (0·51, 0·60)	9·78
M_{ap}/M_{exp}	—	0·95

flexural behaviour of the panels in compression. However, the approximate method predicts also the tripping of the stiffeners of the deck panel. The tripping strength of this stiffened panel is 0.63 and the predicted ultimate bending moment of the ship hull falls to 6.94 MN.m without considering the effect of residual stresses.

The code also allows access to the stress distribution in the section. When the hull is in sagging and the curvature imposed corresponds to the collapse, the neutral axis is located above the bilge, descending towards the bottom. It

is possible to identify a wide zone yielding in tension at the bottom and all the deck is buckled, as well as the upper part of the side.

It is remarkable how low the stresses in the deck are at that level of curvature, less than half of the yield stress. In fact, the first change in the derivative of the curve $M(C)$ corresponds to the collapse of the deck panel and from that curvature a sharp decrease in the deck stresses is observed.

The maximum strain is of 1.88 ε_o and is located at the deck in compression which is much larger than the strain at the keel, 1.19 ε_o in tension. This difference may give an idea how the neutral axis has approached the keel, since, initially, it was nearer to the deck than to the bottom.

4 COMPARISON WITH OTHER NUMERICAL METHODS

Several methods have been applied to the cross sections mentioned above. Finite elements methods were used by Dow[18] while approximate methods were developed by Yao & Nikolov[20] based on Smith's procedure[2] but using an approximate method to predict the average stress-average strain relationship of the stiffened plate elements, by Ueda & Rashed,[21] Paik[22] and Hansen,[23] who has also compared his approximate method with a non-linear finite element code for some cross sections.

The compilation of the results obtained by these methods is summarised in Table 5 and compared with the present method.

The values of the predicted ultimate bending moment are very much the same with exception to the ASAS-NL model from Dow, from the Hansen model without residual stresses and from the model of Yao that gave higher

TABLE 5
Comparison Between Methods of the Predicted Ultimate Bending Moment of the Frigate Model

Method/author	η	*Moment (MN.m)*	%
Experimental	~13	9·78	100·0
Proposed	0	9·61	98·5
Proposed	9	9·31	95·2
ASAS-NL/Dow	—	11·2	114·5
FABSTRAN/Dow	~13	9·56	97·8
ISUM/Paik	17, 12, 6·5	9·68	99·0
HULLST/Yao	~13	10·2	104·3
Hansen	0	11·1	113·5
Hansen	17, 12, 6·5	9·41	96·2

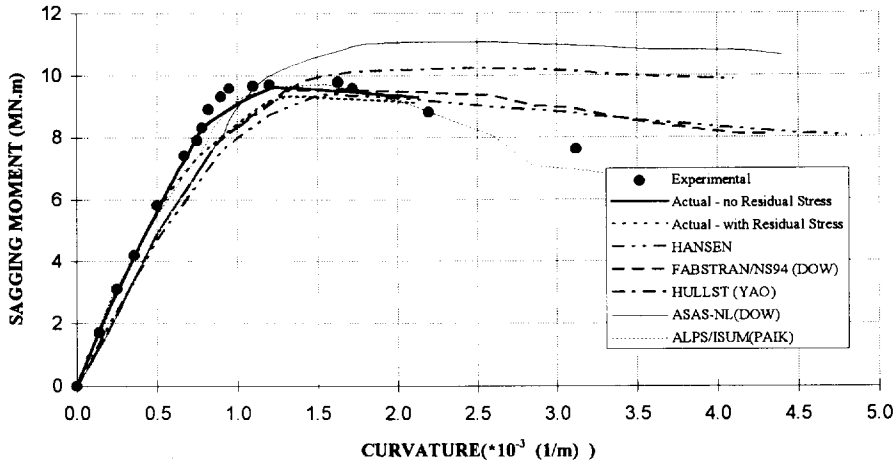

Fig. 14. Comparison of moment–curvature curves of the frigate model from several methods.

values than the others. However, the main differences among the curves are in the pre-collapse regime, as shown in Fig. 14. Most of the methods show an initial rigidity of the cross section lower than in the experiment with the exceptions of the proposed method and of Paik's method. Moreover, all methods are unable to predict the experimental curve near collapse. Here, maybe the problems are related to the derivation of the values near collapse of the experimental data set, as already pointed out.

As concerns the post collapse behaviour of the hull girder, all methods show a similar shedding pattern, in fact slightly lower than the one observed in the experiment. Only Paik obtained a curve close to the experiments in this particular region, but that was achieved by adequately choosing some control parameters on the load-shortening curves of the beam columns which fit this particular case. Since this can only be done in view of the experimental results, its prediction capability does not seem to be better than the other methods.

Finally, the difference in the prediction of the effect of residual stresses on the hull girder response to bending moments must be noted. In the method of Hansen this effect seems to be very important both on the ultimate bending moment (reduction of 15%) and on the shape of the global moment–curvature curve. In the present method there is a delay on the achievement of the ultimate moment but its value varies little (−3.3%) and the post buckling behaviour tends to be the same for all residual stresses levels. This later behaviour is more in agreement with what has been observed in behaviour of plate elements and of stiffened plates.

5 CONCLUDING REMARKS

An approximate method, which has developed in Refs 13 and 14 to model the load shortening behaviour of plate stiffener assemblies, is used to evaluate the behaviour of the hull girder under bending. This model has been extended to represent the behaviour of all elements in a ship cross section and to account for the contribution of each to the bending moment developed in the cross section.

The model predictions have been compared with three independent sets of experiments and very good results were obtained. Most of the experiments are small scale models which is not the best way of testing this approximate method, because the initial assumptions become less applicable when the number of elements belonging to a panel decreases. In spite of this, the experimental results are reproduced with very good accuracy.

However, there are still some problems to be solved when modelling a ship in order to compute the ultimate moment. The dissimilarity of the material properties between the plating and the stiffener as a result of a different manufacturing process has to be solved by some initial assumption because this approximate method and some of finite element programs do not accept different material properties in the same stiffened plate. For example in the experiments of Dowling, table 1, the difference of the prediction may be about 10% when one uses the minimum yield stress instead of the average yield stress.

The predicted tripping strength in the case of some panels is lower than the one expected from the experiments. This certainly means that this theory is somewhat conservative when applied to ship structures, as already pointed out. However, in these small models, some scale problems may play an important role. Finally, the prediction of the model MSC in sagging proves the need of using hard corners in some particular cases. The question that is still open is the particular conditions that must be fulfilled in order to consider one element as a hard corner. In the MSC model the absence of stiffeners in the wing tanks associated with very stocky plating forming a very rigid box seems to be the ideal geometry to obtain an elastic-perfectly plastic behaviour of the whole box, but in the most common cases it is very difficult to judge.

ACKNOWLEDGEMENTS

This work has been performed as part of the research project (B/E 4554) 'Reliability Method for Ship Structural Design (SHIPREL)', which has been partially financed by the Commission of the European Communities under

the BRITE/EURAM programme (Contract no 91-501), and which involves the following additional participants: Bureau Veritas, Germanischer Lloyd, Registro Italiano Navale and Technical University of Denmark.

REFERENCES

1. Caldwell, J. B., Ultimate longitudinal strength. *Trans. Royal Inst. Naval Architects*, **107** (1965) 411–430.
2. Smith, C., Influence of local compressive failure on ultimate longitudinal strength of a ship's hull. In *Proc. Int. Symp. Practical Design in Shipbuilding*, PRADS 77, Tokyo, 1977, pp. 73–79.
3. Kmiecik, M., The influence of imperfections on the load carrying capacity of plates under uniaxial compression. *Ship Tech. Res.*, **39** (1992) 17–27.
4. Faulkner, D., A review of effective plating for use in the analysis of stiffened plating in bending and compression. *J. Ship Res.*, **19** (1975) 1–17.
5. Guedes Soares, C., Design equation for the compressive strength of unstiffened plate elements with initial imperfections. *J. Const. Steel Res.*, **9** (1988) 287–310.
6. Faulkner, D., Adamschak, J. C., Snyder, G. J. & Vetter, M. R., Synthesis of welded grillages to withstand compression and normal loads. *Computers & Struct.*, **3** (1973) 221–246.
7. Guedes Soares, C. & Soriede, T. H., Behaviour and design of stiffened plates under predominantly compressive loads. *Int. Shipbuilding Progress*, **30** (1983) 13–27.
8. Billingsley, D. W., Hull girder response to extreme bending moments. In *Proc. 5th STAR Symp.*, Society of Naval Architects and Marine Engineers (SNAME), 1980.
9. Adamchak, J. C., An approximate method for estimating the collapse of a ship's hull in preliminary design. In *Proc. Ship Structure Symp. '84*, SNAME, 1984, pp. 37–61.
10. Dow, R. S., Hugill, R. C., Clarke, J. D. & Smith, C. S. Evaluation of ultimate ship hull strength. In *Proc. Extreme Loads Response Symp.*, SNAME, 1981, pp. 133–147.
11. Rutherford, S. E. & Caldwell, J. B., Ultimate longitudinal strength of ships: a case study. *Trans. SNAME*, **98** (1990) 441–471.
12. Kutt, L. M., Piaszczyk, C. M., Chen, Y. K. & Lin, D., Evaluation of the longitudinal ultimate strength of various ship hull configurations. *Trans. SNAME*, **93** (1985) 33–53.
13. Gordo, J. M. & Guedes Soares, C., Approximate load shortening curves for stiffened plates under uniaxial compression. *Integrity of Offshore Structures – 5*, EMAS, 1993, pp. 189–211.
14. Gordo, J. M., Guedes Soares, C. & Faulkner, D., Approximate assessment of the ultimate longitudinal strength of the hull girder. *J. Ship Res.*, **40** (1996) (in press).
15. Dowling, J. P., Chatterjee, S., Frieze, P. A. & Moolani, F. M., Experimental and predicted collapse behaviour of rectangular steel box girders. In *Int. Conf. on Steel Box Girder Bridges*, London, 1973.
16. Dowling, J. P., Moolani, F. M. & Frieze, P. A., The effect of shear lag on the

ultimate strength of box girders. In *Steel Plated Structures*, Granada, 1977, pp. 108–141.
17. Nishihara, S., Ultimate longitudinal strength of mid-ship cross section. *Naval Arch. & Ocean Engng*, **22** (1984) 200–214.
18. Dow, R. S., Testing and analysis of a 1/3-scale welded steel frigate model. In *Advances in Marine Structures 2*, (eds C. S. Smith, and R. S. Dow) Elsevier Applied Science, 1991, pp. 749–773.
19. Guedes Soares, C., Uncertainty modelling in plate buckling. *Structural Safety*, **5** (1988) 17–34.
20. Yao, T. & Nikolov, P. I., Progressive collapse analysis of a ship's hull under longitudinal bending (2nd. Rep.). *J. Soc. Naval Arch. Japan*, **172** (1992) 437–446.
21. Ueda, Y. & Rashed, S. M. H., Advances in the application of ISUM to marine structures. In *Advances in Marine Structures 2*, (eds C. S. Smith and R. S. Dow) Elsevier Applied Science, 1991, pp. 628–649.
22. Paik, J. K., Advanced idealized structural elements considering both ductile-collapse and excessive tension-deformation. *Technical Report n. PNUNA-SE-30*, Dep. of Naval Architecture, Pusan National University, Korea, 1993.
23. Hansen, A. M., Strength of midship sections. *Marine Struct.*, **9** (1996).